Overview of the Development of the Solar Electric Propulsion Technology Demonstration Mission 12.5-kW Hall Thruster

Hani Kamhawi[*], Wensheng Huang[†], Thomas Haag[‡], John Yim[§], Li Chang[**], Lauren Clayman[††], Daniel Herman[‡‡], Rohit Shastry[§§], Robert Thomas[***], Timothy Verhey[†††]
NASA Glenn Research Center, Cleveland Ohio

Christopher Griffith[‡‡‡], James Myers[§§§]
Vantage Partners LLC, Cleveland, Ohio

George Williams[****], Ohio Aerospace Institute, Cleveland, Ohio

Ioannis Mikellides[††††], Richard Hofer[‡‡‡‡], James Polk[§§§§], and Dan Goebel[*****]
Jet Propulsion Laboratory, California Institute of Technology, Pasadena, CA

Abstract− NASA is developing mission concepts for a solar electric propulsion technology demonstration mission. A number of mission concepts are being evaluated including ambitious missions to near Earth objects. The demonstration of a high-power solar electric propulsion capability is one of the objectives of the candidate missions under consideration. In support of NASA's exploration goals, a number of projects are developing extensible technologies to support NASA's near and long term mission needs. Specifically, the Space Technology Mission Directorate Solar Electric Propulsion Technology Demonstration Mission project is funding the development of a 12.5-kW magnetically shielded Hall thruster system to support future NASA missions. This paper presents the design attributes of the thruster that was collaboratively developed by the NASA Glenn Research Center and the Jet Propulsion Laboratory. The paper provides an overview of the magnetic, plasma, thermal, and structural modeling activities that were carried out in support of the thruster design. The paper also summarizes the results of the functional tests that have been carried out to date. The planned thruster performance, plasma diagnostics (internal and in the plume), thermal, wear, and mechanical tests are outlined.

Abbreviations

AFRL = Air Force Research Laboratory
ARRM = Asteroid Retrieval and Redirect Mission
GRC = Glenn Research Center
HEFT = Human Exploration Framework Team
HEOMD = Human Exploration and Operations Mission Directorate
JPL = Jet Propulsion Laboratory
MS = Magnetically Shielded

[*] Senior Research Engineer, In-Space Propulsion Systems, hani.kamhawi-1@nasa.gov
[†] Research Engineer, In-Space Propulsion Systems, wensheng.huang@nasa.gov
[‡] Senior Design Engineer, In-Space Propulsion Systems, thomas.w.haag@nasa.gov
[§] Design Engineer, In-Space Propulsion Systems, john.t.yim@nasa.gov
[**] Aerospace Engineer, li.c.chang@nasa.gov
[††] Thermal Analyst, Thermal Systems Branch, lauren.k.clayman@nasa.gov
[‡‡] Project Lead Engineer, In-Space Propulsion Systems, daniel.a.herman@nasa.gov
[§§] Research Engineer, In-Space Propulsion Systems, rohit.shastry@nasa.gov
[***] Research Engineer, In-Space Propulsion Systems, robert.e.thomas@nasa.gov
[†††] Senior System Engineer, In-Space Propulsion Systems, timothy.r.verhey@nasa.gov
[‡‡‡] Senior Mechanical Designer, christopher.m.griffiths@nasa.gov
[§§§] Senior Aerospace Engineer, james.l.myers@nasa.gov
[****] Senior Research Engineer, george.j.williams@nasa.gov
[††††] Principal Engineer, Electric Propulsion Group (353B), ioannis.g.mikellides@jpl.nasa.gov
[‡‡‡‡] Senior Engineer, Electric Propulsion Group (353B), richard.r.hofer@jpl.nasa.gov
[§§§§] Principal Engineer, Propulsion, Thermal, and Materials Systems Group (353L), james.e.polk@jpl.nasa.gov
[*****] Senior Research Scientist, Propulsion, Thermal, and Materials Section (353), dan.m.goebel@jpl.nasa.gov

OES = Optical Emission Spectroscopy
PATT = Performance Acceptance Thermal Test
RPA = Retarding Potential Analyzer
SEP TDM = *Solar Electric Propulsion Technology Demonstration Mission*
STMD = Space Technology Mission Directorate
TDU = Technology Development Unit

1. Introduction

High-power electric propulsion (EP) systems are enabling and enhancing for time-critical missions or missions requiring transportation of large payloads. A number of mission studies were performed over the last decade which highlight the enhancing and enabling features of high-power EP systems for reusable space tug applications for transfer of payloads from low-Earth-orbit to geosynchronous-Earth-orbit and for use in Mars mission scenarios.[1,2,3,4,5]

National interest in high-power EP systems has been renewed. In 2010, NASA's Human Exploration Framework Team (HEFT) concluded that the use of a high-power (i.e., on the order of 300 kW) solar electric propulsion (SEP) system could significantly reduce the number of heavy lift launch vehicles required for a human mission to a near Earth asteroid.[6] Hall thrusters are ideal for such applications because of their high-power processing capabilities and their efficient operation at moderate specific impulses (~2000 s), which leads to reduced trip times for such missions.[7] Recent EP system model estimates that considered factors such as cost, mass, fault-tolerance, cost uncertainty, complexity, ground test vacuum facility limitations, previously demonstrated power capabilities, and possible technology limitations have shown that Hall thrusters operating at power levels of 20-50 kW are strong candidates for human exploration missions operating at total powers up to 500 kW.[8]

NASA's Space Technology Mission Directorate (STMD) is sponsoring the development, maturation, and evaluation of the key technologies needed to reduce the cost and expand the capability of future space exploration activities. One of the projects under STMD is the Solar Electric Propulsion (SEP) project. The SEP project's major development activities are the development of large deployable solar array structures and the high-power EP system (Hall thruster and power processing unit technologies) that can meet NASA's near term science and exploration needs but are also extensible to NASA's future Human exploration needs. The NASA Glenn Research Center (GRC) is partnering with the Jet Propulsion Laboratory (JPL) to carry out the Hall thruster development work. The SEP TDM, initially announced in 2011, is aimed at demonstrating new cutting edge technology in flexible solar arrays and electric propulsion that will increase the maturity of these key SEP technologies for future commercial and government uses. Once these technologies have been demonstrated, they are expected to enable higher performance Low Earth Orbit (LEO) to Geosynchronous Earth Orbit (GEO) transfers as well as a number of other near-Earth orbit transfers and station-keeping maneuvers. These technologies may also benefit a potential robotic mission to redirect an asteroid into cis-lunar orbit for crew exploration. In longer terms, these technologies will reduce mission costs for NASA interplanetary robotic missions in general, and will serve as a precursor to higher power systems for human interplanetary exploration.

Magnetic shielding was enabled by two major events: (1) Aerojet Rocketdyne designed and built the BPT-4000 that demonstrated a zero-erosion state after 5,600 h of qualification testing,[9] and (2) the Jet Propulsion Laboratory (JPL) performed numerical simulations that explained the physics behind these test results.[10] The simulations also explained why erosion of this thruster in the beginning of the life test occurred at rates observed in other Hall thrusters, and why it stopped after material was eroded away to expose a critical magnetic field topology to the plasma. These explanations led to the development of the theory behind magnetic shielding, followed by a laboratory demonstration of the expected reduction of the erosion rates in 6-kW and 20-kW Hall thrusters.[11,12,13] Knowledge gained from applying magnetic shielding circuit design approach in these two Hall thrusters is leveraged in the design and construction of the 12.5-kW Hall thruster.

This paper provides an overview of the 12.5-kW Technology Development Unit (TDU) Hall thruster development activity and the planned thruster test campaign. The paper is organized as follows: section 2 provides an overview of SEP TDM, section 3 presents a brief summary of the NASA-300MS (magnetically shielded) thruster test campaign, section 4 lists the 12.5-kW TDU thruster design specifications, section 5 discuss various aspects of the 12.5-kW TDU thruster design including a summary of the various modeling activities that anchored and supported the thruster design effort, section 6 discusses the thruster test campaign, and section 7 provide a summary of the paper.

2. Solar Electric Propulsion Technology Demonstration Mission

Human and robotic exploration beyond LEO will require enabling capabilities that are efficient, affordable, and reliable. SEP is highly advantageous because of its favorable in-space mass transfer efficiency compared to traditional chemical propulsion systems. SEP stages have the potential to be the most cost effective solution to perform beyond LEO transfers of high mass payloads for human missions. Recognizing that these missions require power levels more than 10 times greater than current electric propulsion systems, NASA embarked upon a progressive pathway to identify critical technologies needed and a plan for a SEP TDM. A 30-kW class SEP TDM is currently in pre-Phase A formulation focused on demonstration of the technologies, operational challenges, and vehicle-level SEP integrated system at a power level that is a significant increase beyond current SOA and an extensible step toward higher power capability for human exploration. The four top-level objectives of the SEP TDM Project, detailed in References 4, 5, and14, are as follows:

- Perform an in-space demonstration that advances the maturity of high-power EP technology and high-power solar array power system technology in relevant space environments and operational regimes;
- Demonstrate integrated SEP spacecraft design, fabrication, and test as well as operational modes associated with orbit transfer;
- Demonstrate extensible high-power EP and solar array power system technologies and integrated SEP spacecraft operational modes that can be adapted for use in next-generation, higher power SEP systems; and
- Provide a SEP-based transportation capability with performance advancements over those previously demonstrated.

The SEP TDM pre-Phase A activities have included the development and evaluation of a total of 17 mission concepts. NASA has developed 8 in-house concepts involving different stakeholders/partners with varying mission costs and technical merit.[4,5,14] Seven mission concepts were developed under contract by industry under Broad Area Announcement (BAA) and Space Act Agreement (SAA) contracts. Two joint NASA-industry mission concepts were developed under Space Act Agreements. All of the mission concepts were evaluated based upon cost, risk, and technical merit against the SEP TDM objectives. Those results, along with cost-sharing partnership discussions, are guiding the implementation approach for the SEP TDM as it transitions to Phase A. One of the NASA in-house concepts is the Asteroid Redirect Robotic Mission (ARRM) involving a partnership with the STMD and Human Exploration and Operations Mission Directorate (HEOMD). The ARRM concept uses a robotic spacecraft equipped with a high power, SEP system to rendezvous with, capture, and redirect a small asteroid with a mass of up to 1000 tons to a long-term stable lunar orbit.[15] Figure 1 shows a rendering of a conceptual ARRM vehicle.[15] The ARRM concept would be enabled by high-power SEP. Because ARRM is enabled by high-power solar array and EP technologies, it is an ideal platform to meet the needs of STMD's SEP TDM. ARRM would demonstrate deployment and operation of a new class of large, lightweight, high-specific-power, flexible-blanket solar arrays in space along with the operation of a high-power, high-performance EP system. As such STMD is also making investments in critical power technologies required for high-power SEP. The Solar Array System contracts are developing two different 15-kW to 25-kW solar array wing technologies that are extensible to higher power.[16]

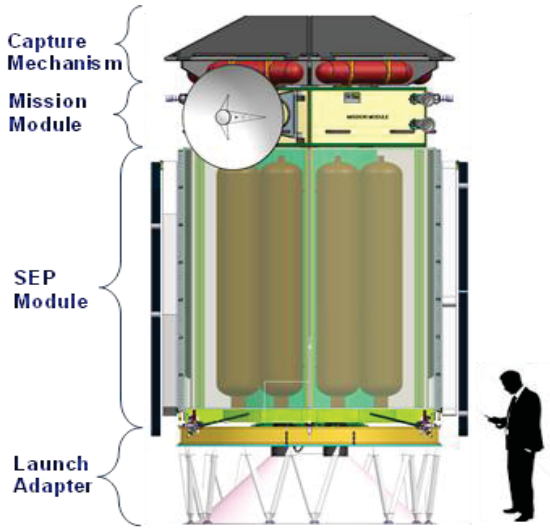

Figure 1. Asteroid Retrieval Vehicle capable of storing up to 10 tons of xenon is shown with the solar array in the stowed configuration.[15]

3. NASA-300 Magnetically Shielded Thruster Test Summary

For NASA SEP TDM candidate missions, the required thruster operating power and throughput capability requires thruster power and lifetime levels that are beyond SOA. To reduce the risk of implementing magnetic shielding on the 12.5 kW TDU Hall thruster, magnetic shielding was incorporated into an existing 20-kW class

Hall thruster, namely the NASA-300M (thereafter referred to as 300M). This was essential because magnetic shielding technology is key to achieving the required thruster lifetime (i.e, propellant throughput) for the candidate SEP TDMs. Another objective was to quantify the change in the thruster performance due to modifying the baseline magnetic field topology of the thruster to a magnetically shielded topology.

In January of 2013, the NASA GRC and JPL team began implementing design changes to the 300M thruster magnetic circuit to demonstrate magnetic shielding. Post modification, the thruster was referred to as the NASA-300 MS (thereafter referred to as 300MS). The methodology employed to modify the original design of the 300M Hall thruster followed closely that used in a recent effort at JPL that led to the demonstration of magnetic shielding in a 6 kW laboratory Hall thruster referred to as the H6MS[10,11,17] The physics-based 2-D axisymmetric plasma code Hall2De[18] was used to guide modifications to the magnetic circuit of the 300M. The plasma simulations were combined with modeling of the magnetic circuit at NASA GRC. The modeling effort produced a magnetically shielded configuration. The experimental setup is similar to one reported in Reference 13.

To preserve the original 300M magnetic configuration, new magnetic circuit components were added to the existing 300M magnetic circuit components in order to attain a magnetically shielded field topology. For the test campaign that is summarized in this paper, two 300MS thruster configurations were evaluated. Configuration 1, designated 300MS, incorporated the magnetically shielded field topology and preserved the discharge channel aspect ratio of the original 300M. Configuration 2, designated 300MS-2, had the same magnetic field topology as the 300MS with the only difference being that the discharge chamber was shortened by 20 percent to investigate the effect of shortening the discharge chamber on thruster performance. The pressure reading, corrected for xenon, next to the thrust stand was less than 3.5×10^{-3} Pa (2.6×10^{-5} Torr) throughout testing.

A number of plasma diagnostics were implemented during this test campaign including:

- Surface flush-mounted Langmuir probes as well as a cylindrical Langmuir probe.[19] The flush-mounted Langmuir probes were used to determine the electron temperature and plasma potential on the chamfered portion of the inner and outer channel surfaces near the thruster exit plane. The cylindrical probe was primarily used to measure the spatial variations in electron temperature within and just downstream of the thruster channel on the 300MS configuration. The probe was mounted on a high-speed axial reciprocated probe system. The cylindrical probe plasma measurements were used to help validate the Hall2De simulation results.
- Far-field Langmuir probe, retarding potential analyzer (RPA), and an ExB probe were mounted on a probe tower with accompanying shielding and shutters protecting the RPA and the ExB probe.[20] This far-field probe tower was attached to a vertical motion stage located ~27 mean thruster diameter downstream of the thruster exit plane, behind a body shield. A NASA GRC designed far-field Faraday probe was used to measure ion current density. It was mounted onto a commercially available three- axis belt-driven motion system. The motion system provides 2D rectilinear motion and probe rotation. The Faraday probe was set at 5 mean thruster diameter away from the thruster because it needed to be far enough away from the thruster for the source of the thruster exhaust to be considered a point source.

Figure 2 shows photographs of the 300MS at the beginning of the test campaign, after 49 hours, and after 99 hours of accumulated operation. From Fig. 2, the image taken after 49 hours shows the inner and outer discharge walls are visibly much darker than at the beginning of the test. Figure 2 also shows that after 99 hours the discharge channel walls are even darker than at 49 hours due to the additional deposition of back sputtered materials.

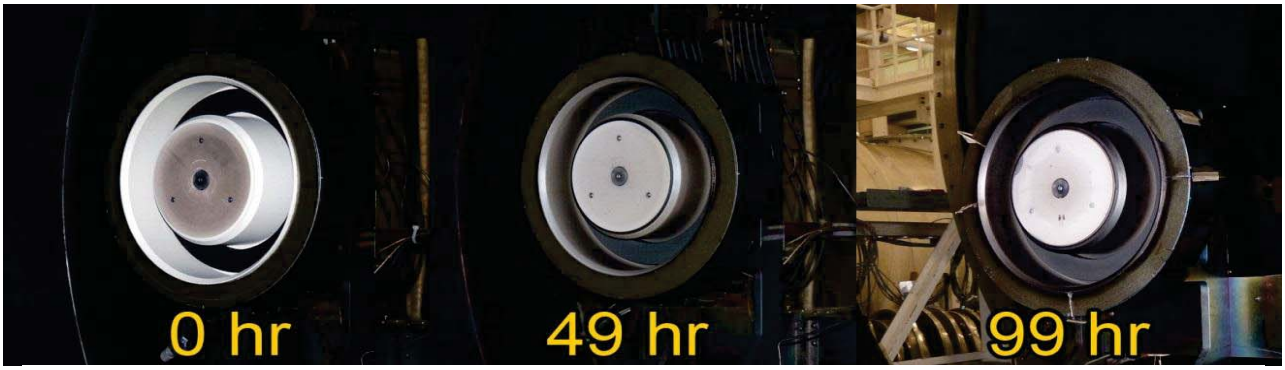

Figure 2. Photographs of the 300MS thruster inside NASA Glenn's VF5 prior to test initiation (left), after 49 hours (middle), and after 99 hours (right).

Definitive confirmation that magnetic shielding was achieved in the 300MS was obtained from the discharge channel wall probes. Detailed analysis of the surface flush-mounted Langmuir probes data is presented by Shastry, et al.[19] Results presented in Table 1 indicate that the plasma properties between the inner and outer surfaces are highly consistent. For all operating conditions, measured plasma potentials (always referenced to cathode potential) are slightly higher than anode potential. This indicates that ions near the discharge channel surfaces will have a negligible amount of beam ion energy. The results in Table 1 confirm that magnetic shielding was achieved.

Table 1. Measured plasma potentials at the inner and outer walls of the 300MS.

	Plasma Potential, V	
Operating Condition	*Inner Wall*	*Outer Wall*
300 V, 10 kW	310	305
300 V, 15 kW	311	304
400 V, 15 kW	410	402
400 V, 20 kW	413	408
500 V, 20 kW	508	501
600 V, 20 kW	600	603

One of the main objectives of the test campaign was to evaluate the performance of a 20 kW-class magnetically shielded Hall thruster to assess whether magnetic shielding results in any thruster performance loss. To complete this assessment and to gain a better understanding of potential loss mechanism that may arise in this new magnetically shielded thruster configuration, thrust measurements and detailed far-field plume measurements were made to elucidate the thruster's performance and loss mechanisms. A detailed presentation of the 300MS and 300MS-2 performance and far-field plume measurements and analysis can be found in References 13 and 20. For this test campaign the performance of the 300MS was conducted at power levels between 2.5 and 20 kW. Tests were performed at discharge voltages of 300, 400, 500 and 600 V. For the 300MS-2 configuration, tests were also performed at discharge voltage of 650 and 700 V to characterize performance at high discharge voltages.

Results reported in Ref. 13 indicate that, in general, for 300 and 400 V thruster operation the 300M performance was higher than the 300MS and the 300MS-2 for power levels above 12.5 kW, whereas for 500 and 600 V thruster operation the 300M performance was higher than the 300MS and 300MS-2 for all power levels. Table 2 below lists the peak total thruster efficiency and specific impulse for the 300M, 300MS, and 300MS-2 thrusters at the different operating discharge voltages. Results indicate that thruster total efficiency and specific impulse for the unshielded and shielded configurations is very similar. Shortening of the discharge channel of the 300MS by 20% did not adversely impact the performance of the magnetically shielded thruster. Far-field plasma probe measurements (Ref. 20) found that, in general, the magnetically shielded configuration had a higher beam divergence than the baseline 300M configuration. This is attributed to the fact that the peak radial magnetic field in the shielded configuration was moved downstream from its baseline location in the 300M, causing the ionization and acceleration zones to shift downstream. The far-field probe data, also found that the 300MS plume charge state was higher than the 300M. This is attributed to the fact that in a magnetically shielded thruster the ion flux to the chamber walls is greatly reduced which causes the electron temperatures along the discharge chamber centerline to reach higher temperatures when compared to an unshielded thruster.[11,12] The higher electron temperatures are attained due to the reduced cooling effects that are derived from the secondary electron emission from the ceramic discharge chamber walls.[21, 22, 23]

Table 2. Summary of the 300M, 300S, and 300MS-2 total efficiency and specific impulse performance at peak power for the various operating discharge voltage magnitudes.

Discharge Voltage, V	Discharge Power, kW	300M		300MS		300MS-2	
		$\eta_{T,\%}$	$I_{sp,T}$, s	$\eta_{T,\%}$	$I_{sp,T}$, s	$\eta_{T,\%}$	$I_{sp,T}$, s
300	15	62	2,010	60	2,090	60	2,120
400	20	66	2,440	64	2,420	63	2,440
500	20	66	2,700	64	2,700	64	2,700
600	20	65	2,910	63	2,880	64	2,880
700	20					63	3,050

4. Design Specifications of the 12.5-kW Technology Development Unit Hall Thruster

NASA GRC has a long history of developing and testing of high-power Hall thrusters in its world-class large high pumping speed vacuum facilities. NASA GRC's high-power Hall thruster research and development efforts started in 1997 with the award of the T-220 10 kW Hall thruster development contract to TRW, Space Power Inc., and the Keldysh Research Center.[24,25] Since then NASA GRC has been involved with testing and/or design of numerous high power Hall thrusters that include the NASA-457Mv1 (50 kW), NASA-400M (40 kW), NASA-300M (20 kW), NASA-457Mv2 (50 kW), Busek's BHT-20k, and Aerojet-Rockedyne's XR-12.[26, 27,28,29,3031,32,33,34,35,36] NASA GRC's and JPL's extensive experience with performance testing, and ion (gridded and non-gridded) thrusters near and far-field plasma measurements is being leveraged in support of the development of a long-life high-performing Hall thruster for NASA's SEP TDM.

The successful test campaigns of the H6MS and the 300MS resulted in the NASA GRC and JPL team adopting magnetic shielding as the design approach for mitigating discharge channel erosion as a life limiting mechanism in the TDU Hall thrusters that are being designed for SEP TDM. In 2013 the NASA GRC and JPL Hall thruster team were focused on designing, fabricating, and testing a 15 kW class long-life high performance 2,000 s capable Hall thruster. The thruster was being designed to demonstrate a technology development unit that can operate at three times the SOA power level with propellant throughput and performance capability that would meet a number of candidate NASA SEP TDM mission needs. Table 3 below summarizes the main attributes of the thruster. The thruster design effort included performing detailed thermal and structural analysis to confirm that design will meet the environmental design attributes (specifications) for potential candidate SEP TDMs. The NASA GRC and JPL design team completed the magnetic, plasma, thermal, and structural modeling of the thruster design. To address the expanded mission options being developed for SEP TDM, such as ARRM, the design team was redirected to design a 12.5 kW Hall thruster with specific impulse capability of 3,000 s. Table 3 summarizes the key thruster design attributes. The major technology push with the TDU thruster design is being able to operate at 12.5 kW up to a specific impulse of 3,000 s with a throughput capability of over 3,300 kg of xenon.

5. 12.5 kW Technology Development Unit Hall Thruster Design and Modeling Methodology

The 12.5-kW TDU thruster design activity leveraged the extensive JPL H6MS and NASA GRC 300MS thruster design and test experiences. The thruster scaling was based on heritage NASA Hall thruster designs. Three candidate thruster heritage configurations were evaluated. Key down select criteria included the throughput capability and performance characteristics of all three configurations. Other selection criteria being considered included: magnetic circuit margin against saturation, volume and thermal margin for the inner magnetic circuit, and thruster configuration heritage. This section will provide a summary of the modeling activities that were carried out for the selected baseline TDU thruster configuration.

Table 3: 15 kW and 12.5 kW Hall Thruster Design Attributes Summary

Thruster Attribute	15 kW Hall Thruster Attribute	12.5 kW Hall Thruster Attribute
Nominal Power, kW	15 kW	12.5 kW
Discharge Voltage, V	200- ≥400 V	200-800 V
Discharge Current, A	≤50 A	≤31 A
Performance: Total Thrust Efficiency & Specific Impulse	≥ 55% @ BOL ≥ 2,000 s @ BOL	≥ 60% @ BOL ≥ 3,000 s @ BOL
Xenon Throughput, Kg	≥ 3,300	≥ 3,300
Specific Mass, kg/kW	≤ 3 kg/kW	≤ 3 kg/kW
Environmental- Thermal	• Inner solar system operations with any sun angle/distance relationship at 0.7 AU • Deep space facing at up to 3.0 AU	• Inner solar system operations with any sun angle/distance relationship at 0.7 AU • Deep space facing at up to 3.0 AU
Environmental- Vibration	Delta IV Launch Load Levels	Delta IV Launch Load Levels

Magnetic and Plasma Modeling:

The methodology employed to design the 12.5-kW TDU thruster followed closely that used in a recent effort at NASA JPL and NASA GRC that led to the demonstration of magnetic shielding in the 6-kW H6MS and the 20-kW class 300MS Hall thrusters[11,12,13,37] The physics-based 2-D axisymmetric plasma code Hall2De[18] has been used to guide the magnetic circuit design of the TDU thruster. The plasma simulations were combined with modeling of the magnetic circuit using a commercially available electromagnetic field simulation software. The modeling effort investigated three magnetically shielded thruster configurations that were based on NASA heritage thruster designs. The plasma simulations, along with other selection criteria as outlined previously, were used to down-select to the TDU thruster baseline configuration. Figure 3 shows the Hall2De computed plasma potential and electron temperature contours for the TDU thruster operating at 12.5 kW and a discharge voltage of 800 V. The results in Fig. 3 indicate that anode potential and low electron temperature are present along the discharge chamber inner and outer boron nitride walls, which results in reduced ion kinetic energy, reduced ion sheath energy, and reduced ion flux to these surfaces. The Hall2De simulation results were then used to compute the projected discharge channel erosion. It was found that the erosion rates were 100 to 1000 times lower than SOA. As such, the magnetic and plasma modeling of the baseline configuration indicated the TDU thruster would be capable of processing greater than 3,300 kg of xenon and will achieve total thruster efficiency and specific impulse above 60% and 3,000 s, respectively.

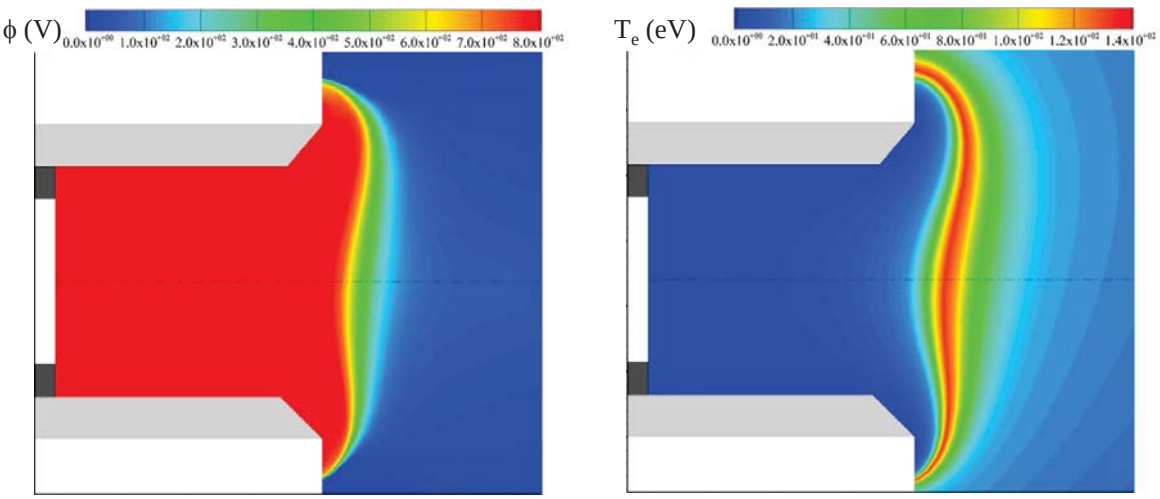

Figure 3. Hall2De predicted plasma potential and electron temperature contour plots for the TDU thruster at a discharge power of 12.5 kW and a discharge voltage of 800 V.

Thruster Design

The TDU thruster baseline configuration, as outlined by the plasma and magnetic simulations, guided the TDU thruster mechanical design. The TDU thruster magnetic circuit model provided the dimensions of the various thruster magnetic circuit components and the discharge chamber. The thruster design leveraged NASA GRC's experience and lessons learned with the design of the NASA-457Mv1&v2, NASA-300M, NASA-120, NASA-173, and HiVHAc. Some of the unique TDU thruster design features include (Figure 4):

- A monolithic boron nitride (BN) discharge chamber;
- A magnetically shielded magnetic field topology;
- A reverse flow propellant manifold with enhanced flow uniformity and protection from backsputtered materials deposition;
- A design capable of withstanding the projected structural and thermal loads for a range of NASA TDMs; and
- A centrally mounted cathode.

Two hollow cathode assemblies were designed for the TDU thruster and they are (Figure 5):

- Assembly 1: Uses a barium oxide (BaO) impregnated porous tungsten thermionic emitter. This assembly design is based on the discharge cathode design for NASA's Evolutionary Xenon Thruster (NEXT) that has recently completed over 50,000 hrs of operation;[38] and
- Assembly 2: Uses a lanthanum hexaboride (LaB6) emitter that has been used on the flight SPT-100 and PPS-1350 thrusters and used in the H6MS thruster. Use of LaB6 emitter eases handling assembly requirements and reduces the propellant purity requirements.[39] However, the LaB6 emitter operates at higher peak temperatures than the BaO impregnated emitter and will require the qualification of new U.S. made heaters.

Figure 4. Photograph of the 12.5-kW TDU thruster.

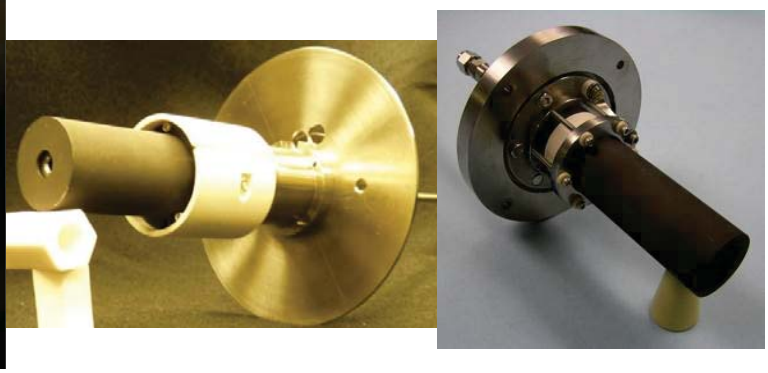

Figure 5. Photographs of hollow cathode assembly 1 (left) and assembly 2 (right).

Propellant Manifold Design and Modeling

The TDU thruster propellant manifold design is intended to provide sufficient azimuthal flow uniformity, attain improved protection against contamination from back-sputtered materials, and optimize manufacturability. A quasi-1D continuum flow analysis was used to size the plenum flow to reduce azimuthal flow non-uniformity. The plenum cross section profile was optimized to reduce the azimuthal pressure delta and to minimize the number of baffle orifices. Direct Simulation Monte Carlo (DSMC) analysis was used to optimize the downstream flow uniformity and to balance the inner and outer flow. Figure 6 shows a normalized pressure profile in the TDU thruster discharge chamber.

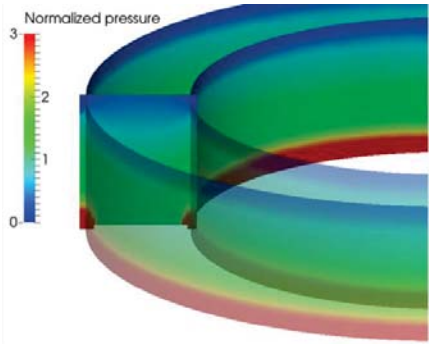

Figure 6. Normalized pressure distribution in the TDU thruster as predicted by the Direct Simulation Monte Carlo.

Thermal Modeling

Thruster

A thermal model of the TDU thruster was developed and used to assess the thermal condition of the design. Similar efforts have been conducted on existing laboratory model Hall thrusters, including the 20-kW 300M and the 50 kW NASA-457Mv2 thrusters.[40] These previous modeling efforts and associated test data provided a basis and level of confidence for this current thermal analysis effort.

The thermal model of the thruster was created in a commercially available 3D finite difference/finite element thermal analysis tool.[41] The thruster geometries for the model were natively recreated within the model for greater control and flexibility. The cathode was not incorporated in the thruster's thermal model, but was modeled separately at NASA JPL. Material properties, both thermophysical and optical, were incorporated into the model as appropriate. The number of nodes defined for each thruster component was based on previous modeling experience to capture the thermal gradients without incurring excessive computational times.

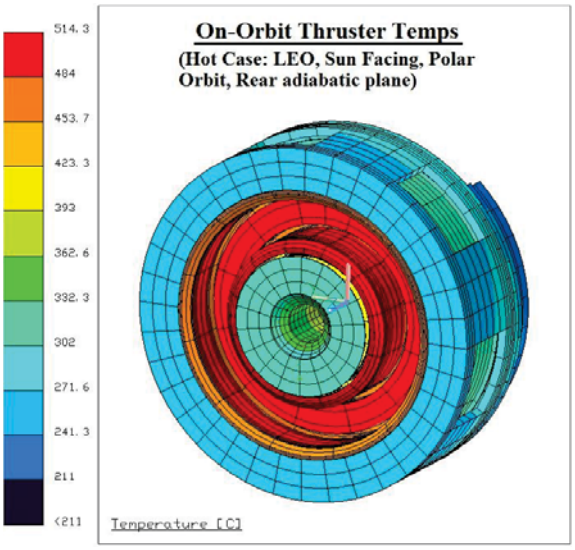

Figure 7. TDU Thruster sample thermal model results.

Heat loads are imposed on the Hall thruster by three main sources during operation: the cathode, the electromagnets, and the discharge plasma. The cathode thermal model provided estimates of the heat flux from the cathode that were then uniformly applied to the thruster surfaces facing the centrally-mounted cathode. The cathode thermal model estimated that roughly 30 W being radiated from the cathode. It is expected that cathode heat output will depend on cathode type, design, and discharge current. The self heating of the electromagnets and heat input from the discharge plasma is important to assess accurately as the electromagnets are one of the more temperature limited components on a Hall thruster. Self-consistent electromagnet currents, wire resistance, and energy output were calculated in a detailed submodel that accounted for conduction across wire, insulation, and potting compound. At the maximum electromagnet current settings, a heat load on the order of 100 W is estimated for the electromagnets.

The heat generated by the discharge plasma dominates the overall thermal condition of the TDU thruster. The heat transfer from the discharge plasma to the thruster anode and discharge channel walls is dependent on a variety of factors including thruster geometry, wall material, discharge voltage, discharge current, and magnetic field shape and strength. Thruster simulations using the Hall2De code were used to provide the heat flux profile to the anode and discharge chamber walls, similar to work done for previous Hall thrusters.[42] The total heat to the anode and discharge walls from the discharge plasma is estimated to be around 1 kW for an 800 V, 12.5 kW operation point, or approximately 8% of the discharge power.

The model assessed the thermal condition of the thruster in both ground test and on-orbit environments. Sample results for one of the on-orbit cases are shown in Figure 7. It was found that the thermal condition of the thruster is driven mostly by internal conditions and not by the external environment. A maximum increase of 11 °C was seen between a thruster operating in a room temperature ground vacuum test facility versus one in orbit in full sun at 1 AU. All components of the thruster were observed to remain below their specified temperature limits. Forthcoming testing of the thruster will provide temperature data to help anchor the model and provide further confidence in the results.

The thermal model of the hollow cathode included all hollow cathode assembly components including the LaB6 emitter, cathode tube, radiation shield, keeper tube, and all the mounting interfaces. The cathode thermal model included the thruster's inner core and the back pole as fixed temperature components. Detailed cathode heat flow maps were generated for various heater power operating powers and emission currents. Results from the cathode thermal model were provided as input for the thruster's thermal model. Figure 8 shows a 45^{o} slice of the cathode axisymmetric thermal model.

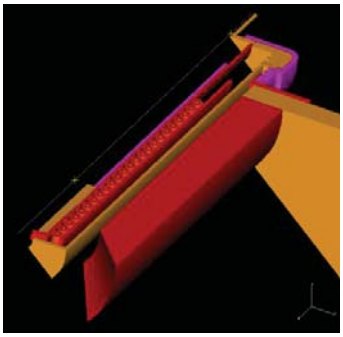

Figure 8. 45° slice of cathode axisymmetric thermal model.

Structural Modeling

A number of structural analyses were performed on the thruster design including modal, limit load stress, thermally-induced stress, and fastener analyses. Additional structural concerns, such as acoustic and shock loads were not specifically analyzed at the thruster level. For acoustic loads, they are typically a concern mainly for components with a large surface area and a thin cross section. However, Hall thrusters are rather compact, solid devices and thus it was assumed that acoustic loads would likely not be an issue, but should be assessed in further detail for future flight development. Shock loads at the thruster interface were also assessed by accounting for source shock attenuation through a representative spacecraft configuration. The resulting qualification level (with a +6dB margin) shock loads were found to lie well below 50 in/s velocity criteria that is typically used as a preliminary limit for failure for electronic equipment.[43] The Hall thruster design does include a large brittle ceramic BN discharge channel, which may need to be investigated further from a shock load standpoint to see if there is still risk of damage.

The structural modes of the thruster were assessed to determine the shapes and frequencies of the first few modes. The ability of a finite element model to capture the modal response frequencies provides a level of confidence in the model to represent the dynamic behavior of the thruster. Past work on the 50 kW NASA-457Mv2 thruster has shown good correlation of the model modal results to measured test values. The model results were found to generally lie within the frequency range of the different test data for the first four modes, and within 5% of at least one test result as prescribed in NASA-STD-5002. The same approach in creating and applying the finite element model is used here for the 12.5-kW TDU thruster.

The structural model of the thruster was developed with the ANSYS Workbench platform, a commercially available software program for static and dynamic structural evaluations. The thruster geometry was imported from a simplified CAD model. The model consisted of over 600,000 nodes and 300,000 elements. Boundary conditions were applied to the base of the mount ring. The thruster is expected to fasten to the gimbal through this surface and loads are transferred at this location. The first few mode shapes and frequencies are presented in Table 4. The fundamental frequency of the thruster is over 600 Hz, which is relatively high. Typically frequencies above 70 Hz are not a concern for integration, thus no issues with the thruster modal response is expected. However, this would be confirmed with the launch vehicle and spacecraft for a future flight mission.

Table 4: Modal analysis results.

Mode	Frequency [Hz]	Shape
1	610	Lateral bending (rocking) mode
2	630	Axial translational (bounce) mode
3	1080	Secondary lateral bending (rocking) mode

This same model was used to calculate estimated stress levels from launch loads and thermal expansion. The areas of highest stress in the design reside in the back pole and the mount ring, but remained below 10 ksi, as shown in Figure 9. Positive margins were found for all major structural components of the thruster. Fastener analyses for the joints on the thruster were also assessed for launch loads and thermally-stressing conditions. The thruster design was found to have sufficient positive margins regarding material tensile strength, bolt separation, and various shears and bearing loads. Overall, the thruster design is expected to be structurally sufficient with positive margins regarding the stressing cases for the aspects examined.

Two TDU thrusters are being fabricated at NASA GRC. TDU1 thruster fabrication was initiated in February of 2014 and was completed in June of 2014. TDU2 thruster fabrication is anticipated to be completed in August of 2014.

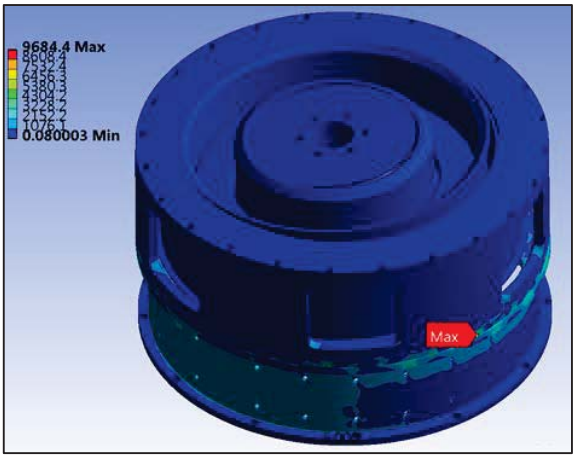

Figure 9. Sample stress results from the structural model of the TDU thruster

6. 12.5 kW Technology Development Unit Thruster Test Plan

The TDU thrusters will be subjected to an extensive set of tests to evaluate the thruster performance, throughput capability, and ability to withstand the range of specified thermal and structural loads that are required for the various candidate SEP TDMs. TDU1 thruster is being tested at NASA GRC. TDU2 will undergo functional and performance acceptance testing at NASA GRC and will then be shipped to JPL to undergo an extensive set of environmental (random vibration and thermal vacuum) tests, and then will undergo additional detailed performance and plasma characterization.

The thruster test plan for of FY14 is comprised of five test segments as summarized below:

1. **Functional Tests:**

Thruster functional tests are underway to confirm the thruster's magnetic field topology, propellant manifold discharge chamber azimuthal flow symmetry, and voltage isolation capability of the thruster. These tests included:

Magnetic Testing:

The TDU thruster magnetic field topology was mapped at various electromagnetic operating currents. Magnetic mapping measurements were performed to confirm that the thruster magnetic circuit is magnetically shielded and that the required magnetic field strength is achieved at the allowable peak electromagnet current settings. Mapping results indicated that a magnetically shielded field topology was attained and that at the maximum design electromagnet current settings the radial magnetic field strength was 30% higher than the peak radial magnetic field strength that is projected for thruster operation at a discharge voltage of 800 V as informed by the H6MS tests, 300MS tests, and Hall2De simulations.

Propellant Manifold Discharge Chamber Flow Measurements:

The radial and azimuthal flow uniformity in the TDU thruster chamber was assessed by measuring the neutral density with an ion gauge. The TDU1 thruster discharge chamber was placed on a rotary stage, and two linear stages were used to translate the pressure probe in the axial and radial directions. Figure 10 shows a photograph of the test setup. Measurements were made at 16 evenly spaced azimuthal locations, at each azimuthal location the neutral density in the axial –radial plane was measured with 3 axial and 7 radial evenly-spaced positions. Tests were performed at flow rates of 7.5, 11.25, 15, 22.5, and 30 mg/s. The data obtained from this test are being analyzed and are being compared to the propellant manifold modeling results. Once thruster performance tests are completed the thruster design team will determine acceptable flow uniformity criteria.

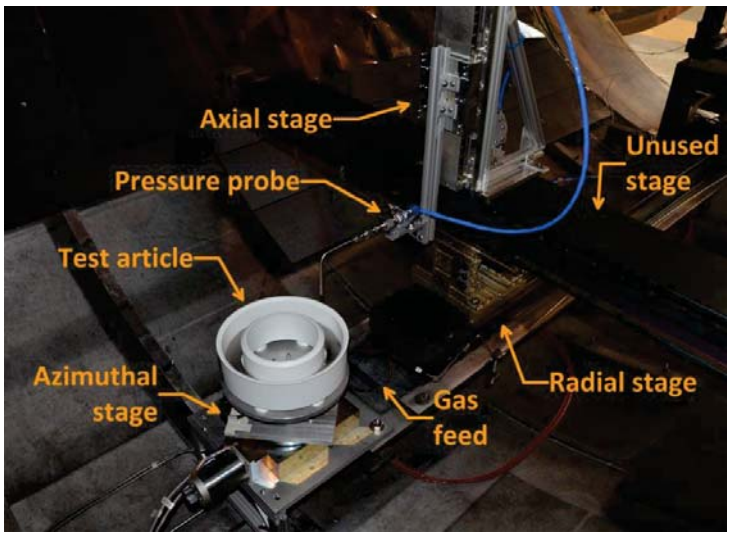

Figure 10. Photograph of the TDU thruster discharge chamber flow uniformity test setup.

Voltage Isolation Tests:

A high voltage megger was used to confirm that the TDU1 thruster is capable to operating at discharge voltage of 800 V. Voltage isolation tests confirmed that the voltage isolation between the anode-cathode, anode-thruster body, thruster body-electromagnet leads was greater than 100 MΩ.

Hot Fire Functional Tests:

The A hot-fire functional test will be performed in NASA GRC's vacuum facility 12 (VF12) at power levels of up to 9 kW and at discharge voltages up to 800 V. The main objectives of the test are to confirm

the thruster's ability to operate in vacuum and to confirm that no voltage breakdowns occur during thruster operation. The thruster performance will be measured to provide an initial assessment of the thruster's thrust efficiency and specific impulse. Upon completion of the VF12 hot fire test, the thruster will be disassembled and the various thruster components will be inspected.

2. **Performance Acceptance and Thermal Test (PATT):**

The performance of the thruster and temperatures of key thruster components will be measured in vacuum facility 5 (VF5). Tests will be performed at power levels between 600 W to 12.5 kW at discharge voltages between 200 and 800 V with the peak discharge current limited to approximately 31 A. High specific impulse and high thrust-to-power throttle tables will be generated and will be used to refine candidate SEP TDM analyses. Temperature measurements of key thruster components (as informed by the thermal model) will be made during testing. Near-field Faraday, RPA, Langmuir and E×B probe measurements will also made. The plasma probe setup is similar to previous test setup but has been improved to enable measurements behind the thruster's exit plane. A quartz crystal microbalance will be used to monitor the backsputter rate in the proximity of the thruster. Background pressure in the vicinity of the thruster will also be continuously monitored with a number of ion gauges located near the thruster and at various locations in VF5.

Optical diagnostics will also be employed to characterize the surface erosion and near-field plasma of the TDU. Optical emission spectroscopy (OES) will be used to provide a real-time correlation of the erosion of thruster surfaces with thruster operating conditions. The surfaces will include channel walls, pole-piece cover, and cathode keeper. OES will also be used to characterize the electron temperature of the plasma in the near-field through localized measurements and full-field images.[44] In addition, modulated diode laser absorption spectroscopy will be employed with the intension to measure relative densities of Xe I and Xe II in the near field of the plasma. Velocity shifts in the absorption spectrum will yield bulk plasma velocities which may be deconvolved through Airy inversion techniques. The optical diagnostics measurements will be used to validate numerical models which address/predict service life, facility effects, spacecraft interaction, and off-nominal operation.

The tests in VF5 will be the first series of thruster tests that will be performed in the chamber after undergoing a major reconfiguration effort. During the past 12 months, the VF5 cryopanels have been reconfigured to achieve a factor of 2 to 3 increase in the pumping speed at the thruster test location. The VF5 reconfiguration will enable facility background pressure magnitudes during thruster operation that are 2 to 3 times lower than what has been achieved in the past.[45] Recently conducted xenon cold flow tests in VF5 indicated that at least a 2 times improvement in VF5's pumping speed has been achieved. VF5 cold flow test results indicated that a background pressure of approximately 2×10^{-6} Torr (corrected for xenon) will be attained when testing at 800 V and 15.6 A. This improved VF5 pumping speed in the thruster vicinity will better replicate the space environment, thus enabling ground test results to be more representative of the thruster operation in space.

3. **Plasma Properties and Facility Effects Characterization Tests:**

This test segment is directed at understanding how the facility background pressure conditions affect the thruster performance and its operating characteristics (i.e, discharge current oscillations, current-voltage characteristics at various electromagnet settings (IV-B), plasma properties in the discharge and thruster near-field environment, etc). Facility effects on thruster operation and wear mechanisms will be assessed by fully characterizing the thruster performance and plasma environment at different facility background pressure conditions. In addition to the plasma probes and optical diagnostics employed in the PATT, the thruster discharge chamber walls and front pole plasma probes will be used to quantify plasma surface properties and these measurement results will be compared with results from JPL's Hall2De code to confirm that the predicted wear rates of key thruster components are consistent with the projected propellant throughput of the device.

4. **Wear Test:**

At the conclusion of the plasma properties and facility effects characterization test, and after performing preliminary data analysis to verify that the erosion rates of key thruster components are consistent with the projected throughput capability of the thruster, a wear test will be initiated. A select sub-set of the plasma and optical diagnostics that were employed during test segments 2 and 3 will be implemented during the wear test. The wear test will be used to confirm that the erosion rates of key thruster components (namely the BN discharge channel walls and critical magnetic circuit components) are consistent with modeled wear rates and that no unpredicted wear mechanisms are uncovered. It is projected that the wear test will

continue into FY15 and the team is planning to accumulate a few thousands hours of operation at full power on the thruster. This will enable the team to uncover any unpredicted wear mechanisms that have not been predicted by the team.

5. **Environmental Tests:**

Environmental tests of the TDU2 thruster will be performed at NASA JPL. After completing fabrication and an abbreviated PATT of TDU2 at NASA GRC, TDU2 will be shipped to NASA JPL. At NASA JPL the thruster will undergo a random vibration and thermal vacuum tests. The two tests will be performed to confirm that the thruster meets the structural and thermal design specifications that can be derived from the top-level attributes listed in Table 3. Measurements performed during the random vibration and thermal vacuum tests will be compared to structural and thermal modeling results and will help refine the developed models to enable very accurate prediction of thruster characteristics for the various candidate mission scenarios.

6. **Component Testing:**

Standalone tests will be performed on the thruster's hollow cathode assemblies and the inner electromagnet. Hollow cathode assemblies standalone tests include performing tests at both GRC and JPL of assemblies 1 and 2, respectively, to measure the plasma properties in the cathode's plume. Tests at JPL (for both cathode assemblies) will also be performed to measure the emitter temperature and the plasma properties inside the emitter region and along the cathode centerline.[46,47] These detailed internal cathode measurements will be used, in conjunction with simulations using the 2-D axisymmetric Orificed Cathode (OrCa2D) code, to obtain accurate estimates of cathode life.[48,49]

An inner electromagnet test coil was fabricated, and instrumented with over 15 thermocouples. Thermal characterization tests of the test coil, in vacuum, will be conducted to provide detailed thermal measurements at various inner electromagnet layers in for varying electromagnet currents in support of validating the inner electromagnet and thruster thermal models.

7. Summary

NASA's Space Technology Mission Directorate is sponsoring the design, manufacture and testing of a high-power Hall thruster that supports NASA's Human and Science exploration mission needs. NASA GRC and JPL are supporting the Agency's science and human exploration objectives by developing mission concepts for a Solar Electric Propulsion Technology Demonstration Mission. The NASA GRC and JPL team has completed the design and fabrication of a 12.5-kW TDU Hall thruster that meets the specification of a range of SEP TDM candidate missions. The NASA GRC and JPL team has performed detailed magnetic, plasma, flow, thermal, and structural modeling and analysis in support of the thruster design. The modeling and analysis performed to date indicates that the 12.5-kW TDU thruster design is able to meet the performance, propellant throughput, and environmental requirements for a number of candidate SEP TDMs. Two 12.5 kW TDU thruster are being fabricated. TDU1 fabrication has been completed and the thruster is currently undergoing functional testing and will soon undergo performance acceptance and thermal characterization tests. TDU2 thruster fabrication will be completed in August of 2014. The planned TDU1 test campaign will characterize the thruster performance, thermal operation, and plasma properties (internal and in the plume) to demonstrate that the TDU thruster design will meet the performance and throughput design specifications. TDU2 test campaign will initially assess the thruster's design ability to meet the environmental design specifications.

Acknowledgments

The authors would like to thank and acknowledge the Space Technology Mission Directorate for funding this work. The authors thank and acknowledge the support of Timothy Smith, STMD In Space Propulsion project manager. The authors would also like to thank Kevin Blake, Mike Pastel, Kevin McCormick, Richard Polak, and NASA GRC fabrication division for their help in fabricating the 12.5 kW Hall thruster.

References

[1] Dudzinski, L., et al., "Design of Solar Electric Propulsion Transfer Vehicle for a Non-Nuclear Human Mars Exploration Architecture," IEPC Paper 99-181, October 1999.

[2] Oleson, S.R., et al., "Advanced Propulsion for Space Solar Power Satellites," AIAA Paper 99-2872, June 1999.

[3] Oleson, S.R., et al., "Mission Advantages of Constant Power Variable Specific Impulse Electrostatic Thrusters," NASA TM-2000-210477, March 2000.

[4] McGuire, M. L., Hack, K. J., Manzella, D. H., and Herman, D. A., " Concept designs for NASA's Solar Electric Propulsion Technology Demonstration Mission," AIAA-2014-3717, 50th AIAA/ASME/SAE/ASEE Joint Propulsion Conference, Cleveland, OH, July 28-30, 2014.

[5] Manzella, D., and Hack, K., "High-Power Solar Electric Propulsion for Future NASA Missions," AIAA-2014-3718, 50th AIAA/ASME/SAE/ASEE Joint Propulsion Conference, Cleveland, OH, July 28-30, 2014.

[6] http://www.nasa.gov/exploration/new_space_ enterprise/home/heft_summary.html

[7] Brophy, J.R., et al., "300-kW Solar Electric Propulsion System Configuration for Human Exploration of Near Earth Asteroids," AIAA Paper 2011-5514, August 2011.

[8] Hofer, R. R. and Randolph, T. M., "Mass and Cost Model for Selecting Thruster Size in Electric Propulsion Systems," Journal of Propulsion and Power 29, 1, 166-177 (2013).

[9] K.H. De Grys, A. Mathers, B. Welander, V. Khayms, AIAA Paper No. 10-6698, in: Proceedings of the 46th AIAA/ASME/SAE/ASEE Joint Propulsion Conference, Nashville, TN, 2010, pp. 6698.

[10] Mikellides, I.G., Katz, I., Hofer, R. R., *et al.*, "Magnetic shielding of the channel walls in a Hall plasma accelerator," *Physics of Plasmas*, vol. 18, no. 3, pp. 033501, Mar, 2011.

[11] I. G. Mikellides, I. Katz, R. R. Hofer *et al.*, "Magnetic shielding of a laboratory Hall thruster. I. Theory and validation," *Journal of Applied Physics*, vol. 115, no. 4, Jan 28, 2014.

[12] R. R. Hofer, D. M. Goebel, I. G. Mikellides *et al.*, "Magnetic shielding of a laboratory Hall thruster. II. Experiments," *Journal of Applied Physics*, vol. 115, no. 4, Jan 28, 2014.

[13] Kamhawi, H., et al., "Performance and Thermal Characterization of the NASA-300MS 20 kW Hall Effect Thruster," Proceedings of the 33rd International Electric Propulsion Conference, IEPC-2013-444, Washington, D.C., October 6-10, 2013.

[14] Smith, B., Nazario, M. L., and Manzella, D. H., "Advancement of a 30kW Solar Electric Propulsion System Capability for NASA Human and Robotic Exploration Mission," IAC-12-C4.4.2.

[15] Brophy, et. al., "Near-Earth Asteroid Retrieval Mission (ARM) Study," IEPC-2013-082.

[16] Mercer, C., "Advanced Solar Arrays," Plantery Science Division Discovery Technology Workshop, April 2014. http://discovery.larc.nasa.gov/PDF_FILES/02-AdvSolrArry-CMercer-2.pdf.

[17] Mikellides, I.G., Katz, I., Hofer, R.R., and Goebel, D.M., "Design of a Laboratory Hall Thruster with Magnetically Shielded Channel Walls, Phase III: Comparison of Theory with Experiment,"AIAA 2012-3789, July 2012.

[18] Mikellides, I.G, and Katz, I., Numerical simulations of Hall-effect plasma accelerators on a magnetic-field-aligned mesh, *Physical Review E*, 86 (2012) 046703.

[19] Shastry, R., Huang, W., Haag, T. W. and Kamhawi, H., "Langmuir Probe Measurements within the Discharge Channel of the 20-kW NASA-300M and NASA-300MS Hall Thrusters," Proceedings of the 33rd International Electric Propulsion Conference, IEPC-2013-122, Washington, D.C., October 6-10, 2013.

[20] Huang, W., Shastry, R., Soulas, G. C., and Kamhawi, H., "Farfield Plume Measurement and Analysis on the NASA-300M and NASA-300MS", 33rd International Electric Propulsion Conference, IEPC-2013-057, Washington, DC, 6-10 Oct, 2013.

[21] Kim, V., "Main Physical Features and Processes Determining the Performance of Stationary Plasma Thrusters," Journal of Propulsion and Power, Vol. 14, No. 5, Sept.-Oct. 1998, pp. 736-746.

[22] Kim, V., et al., "Investigation of SPT Performance and Particularities of its Operation with Kr/Xe Mixtures," IEPC-01-065, Sept. 2001.

[23] Goebel, D. M., and Katz, I., Fundamentals of Electric Propulsion: Ion and Hall Thrusters, JPL Science and Technology Series, Pasadena, CA, 2008, Chap. 7.

[24] Jankovsky, R.S., et al., "Preliminary Evaluation of a 10 KW Hall Thruster," AIAA Paper 99-0456, January 1999.

[25] Mason, L.S., et al., "1000 Hours Testing of a 10 KW Hall Effect Thruster," AIAA Paper 2001-3773, July 2001.

[26] Jankovsky, R.S., et al., "NASA's Hall Thruster Program 2002," AIAA Paper 2002-3675, July 2002.

[27] Manzella, D. H., et al., "Laboratory Model 50 kW Hall Thruster," AIAA-2002-3676, July 2002.

[28] Peterson, P. Y., "Performance and Wear Characterization of a High Power High–Isp Hall Thruster," AIAA Paper 2005-4243, July 2005.

[29] Jacobson, D.T., et al., "NASA's 2004 Hall Thruster Program," AIAA-2004-3600, July 2004.

[30] Peterson, P. Y., "Performance and Wear Characterization of a High Power High–Isp Hall Thruster," AIAA-2005-4243, July 2005.

[31] Kamhawi, H., Haag, T. W., Jacobson, D. T., and Manzella, D. H., "Performance Evaluation of the NASA-300M 20 kW Hall Effect Thruster", AIAA-2011-5521,July 2011.
[32] Soulas, G. C., Haag, T. W., Herman, D. A., Huang, W., Kamhawi, H., Shastry, R. and Williams, G., "Performance Test Results of the NASA-457M v2 Hall Thruster," AIAA-2012-3940, July 2012.
[33] Herman, D. A., Shastry, R., Huang, W., Soulas, G. C. and Kamhawi, H., "Plasma Potential and Langmuir Probe Measurements in the Near-field Plume of the NASA-300M Hall Thruster," AIAA-2012-4115, July 2012.
[34] Huang, W., Shastry, R., Herman, D. A., Soulas, G. C. and Kamhawi, H., "Ion Current Density Study of the NASA-300M and NASA-457Mv2 Hall Thrusters," *Proceedings of the 48th AIAA/ASME/SAE/ASEE Joint Propulsion Conference and Exhibit*, AIAA-2012-3870, July 2012.
[35] Shastry, R., Huang, W., Herman, D. A., Soulas, G. C. and Kamhawi, H., "Plasma Potential and Langmuir Probe Measurements in the Near-field Plume of the NASA-457Mv2 Hall Thruster,", AIAA-2012-4196, July 2012.
[36] Szabo, J., et al., "A Commercial One Newton Hall Effect Thruster for High Power In-Space Missions," AIAA-2011-3940, July 2011.
[37] Mikellides, I.G, and Katz, I., Kamhawi, H., and VanNoord, J., "Numerical Simulations of a 20-kW Class Hall Thruster Using the Magnetic-Field-Aligned Mesh Code Hall2De," IEPC-2011-244, September, 2011.
[38] Shastry, R., Herman, D. A., Soulas, G. C., and Patterson, M. J., "End-of-test Performance and Wear Characterization of NASA's Evolutionary Xenon Thruster (NEXT) Long-Duration Test", 50th AIAA/ASME/SAE/ASEE Joint Propulsion Conference, Cleveland, OH, July 28-30, 2014.
[39] Goebel, D. M. and Chu, E., "High-Current Lanthanum Hexaboride Hollow Cathode for High-Power Hall Thrusters," Journal of Propulsion and Power 30, 1, 35-40 (2014).
[40] Yim, J. T., Clayman, L. K., and Chang, L. C., "Thermal and Structural Modeling and Analyses of NASA High Power Hall Thrusters," *Proc. Joint Army-Navy-NASA-Air Force (JANNAF) 6th Spacecraft Propulsion Subcommittee Meeting*, Colorado Springs, CO, April-May 2013.
[41] Panczak, T., Ring, S., and Welch, M., "A CAD-based Tool for FDM and FEM Radiation and Conduction Modeling", *SAE Transactions*, Vol. 107, No. 1, 1998, pp. 363–372.
[42] Katz, I., Mikellides, I. G., and Hofer, R. R., "Channel Wall Plasma Thermal Loads in Hall Thrusters with Magnetic Shielding", *47th AIAA/ASME/SAE/ASEE Joint Propulsion Conference and Exhibit*, July 2011, AIAA 2011-6082.
[43] Morse, R., "Velocity as a Potential Pyro-Shock Damage Indicator for Electronic Equipment," *Spacecraft and Launch Vehicle Dynamic Environments Workshop Program*, June 20, 2000.
[44] Williams, G.J., Soulas, G.S., and Kamhawi, H., "Advanced Diagnostic Characterization of High-Power Hall Thruster Wear and Operation," 48th AIAA Joint Propulsion Conference, AIAA Paper-2012-4036, July, 2012.
[45] Yim, J. T., Herman, D. A., Burt, J. M., "Modeling analysis for NASA GRC Vacuum Facility 5 Upgrade," NASA/TM-2013-216496, February 2013.
[46] Polk, J., Marrese-Reading, C., Thornber, B., Dang, L., Johnson, L. and Katz, I., "Scanning Optical Pyrometer for Measuring Temperatures in Hollow Cathodes," Rev. Sci. Inst., 78, 093101, 2007.
[47] Goebel, D., Jameson, K., Watkins, R., Katz, I., and Mikellides, I., "Hollow cathode theory and experiment. I. Plasma characterization using fast miniature scanning probes," J. Appl. Phys., 98, 113302 2005.
[48] Mikellides, I. G., and Katz, I., "Wear mechanisms in electron sources for ion propulsion, 1: Neutralizer hollow cathode," Journal of Propulsion and Power, vol. 24, no. 4, pp. 855-865, Jul-Aug, 2008.
[49] Mikellides, I. G., Katz, I., Goebel, D. A., et al., "Wear mechanisms in electron sources for ion propulsion, 2: Discharge hollow cathode," Journal of Propulsion and Power, vol. 24, no. 4, pp. 866-879, Jul-Aug, 2008.